Soils and Foundations 2016;56(3):574–580

HOSTED BY

ELSEVIER

The Japanese Geotechnical Society

Soils and Foundations

www.sciencedirect.com
journal homepage: www.elsevier.com/locate/sandf

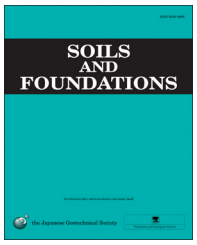

Evaluating use of resonant column in flexural mode for dynamic characterization of Bangalore sand

B.N. Madhusudhan[a,*], K. Senetakis[b]

[a]*University of Southampton, Southampton, UK*
[b]*University of New South Wales, Sydney, Australia*

Received 8 March 2015; received in revised form 28 January 2016; accepted 27 February 2016
Available online 6 May 2016

Abstract

The resonant column method is a well-established medium-frequency wave propagation technique for the dynamic characterization of soils. This study presents an evaluation of Young's modulus of a quartzitic sand derived from flexural resonant column tests. The results are compared with extender elements, which are embedded in the same apparatus and apply high-frequency P-wave propagation, as well as a published model in the literature derived from longitudinal resonant column experiments. The comparison of the elastic Young's modulus values was satisfactory. The material damping derived from the free-vibration decay method had higher values in flexural mode than torsional mode. And, with an increase in confinement, a faster reduction in material damping associated with S-wave propagation was observed. The results of the study are promising for the standardization of the flexural mode of vibration in the classical torsional resonant column device which can provide invaluable insight into the behavior of state and effective stress-dependent materials.

1. Introduction

The resonant column (RC) method provides reliable measurements of the stiffness and damping of geo-materials (Clayton, 2011). In the torsional and longitudinal modes of vibration, the RC technique has been standardized and it allows for the study of the complete dynamic behavior of soils, i.e., shear modulus, Young's modulus and material damping at variable modes of excitation (ASTM, 1992). During resonant column tests, medium-frequency excitation, commonly of the sinusoidal type, is applied to cylindrical samples. By solving the differential equations associated with the wave propagation of elastic waves in prismatic rods, considering appropriate boundary conditions, the basic formulae for the resonant column analysis are derived (ASTM, 1992; Richart et al., 1970).

Advances in the theory and modification of the circuit for exciting coils have rendered the simultaneous determination of the torsional and flexural modes of vibration in the same device with the use of a single drive mechanism (Cascante et al., 1998). This makes the overall configuration simpler in comparison to other types of resonant columns, wherein two different drive mechanisms are used to evaluate the shear modulus and Young's modulus, for example, in the work by Saxena and Reddy (1989). In order to obtain comparable dynamic properties of a soil sample at a given stress state, a single excitation system is necessary and the available literature with such devices is limited. This brief note presents resonant column tests in association with the determination of elastic Young's modulus and damping in the flexural mode of vibration. The results are evaluated with previously published data in which different experimental techniques have been

*Corresponding author.
E-mail address: mbnm1f13@soton.ac.uk (B.N. Madhusudhan).
Peer review under responsibility of The Japanese Geotechnical Society.

http://dx.doi.org/10.1016/j.sandf.2016.04.021

used. Measurements of material damping in torsional and flexural modes of vibration are also obtained and discussed briefly in the paper.

2. Equipment, materials and sample preparation

The poorly graded sand of the sub-angular particles from Bangalore, India was examined in this study. The grading curve for the sand and the scanning electron microscopy image are shown in Fig. 1. The basic properties of the sand are summarized in Table 1. An X-ray diffraction analysis indicated that the primary minerals present in the sand are quartz (80%) and feldspar (20%). The resonant column apparatus (modified Stokoe-type), under cantilever fixed-free end conditions, modified to exert torsional and flexural vibrations to the cylindrical specimen (Cascante et al., 1998), was used for the study. This allowed for the independent measurements of shear modulus (G) and Young's modulus (E) in the range of medium frequencies (e.g., 20–200 Hz) along with the corresponding material damping in torsional mode (D_s) and flexural mode (D_f). The sample end caps house bender/extender elements which can generate and receive P and S waves through the sample in the same apparatus (Kumar and Madhusudhan, 2010), a technique which applies high-frequency dynamic excitation typically in the range of 1–20 kHz. A schematic diagram of the apparatus is shown in Fig. 2. A close-up view of the excitation mechanism with embedded magnets, fixed on top of the sample and the surrounding coils, is shown in Fig. 3. Air was used as the confining medium along with digital air proportion valves to regulate the cell pressure. Thus, the second inner cell, filled with silicon oil, protects against the diffusion of air into the sample through the membrane. Although air diffusion is not important under air-drained conditions, since the samples are dry, an inner fluid cell filled with silicon oil was used for the testing to maintain uniformity of the testing procedure in order to make a comparison with the saturated samples reported elsewhere (Kumar and Madhusudhan, 2011).

The dry sand was air pluviated from a calibrated height to accurately achieve the target relative density (Kumar and Madhusudhan, 2010). This technique provides a reliable method for obtaining a homogenous repeatable sample for any given relative density (Lo Presti et al., 1992). The scheme of the pluviation device composed of a thin-walled cylindrical split mold and the calibration plot derived from trials prior to the resonant column testing are shown in Fig. 4. The sample was prepared at the target relative density and the top cap was placed with a thin layer of vacuum grease between the top cap and the membrane. Suction pressure of 20 kPa was then applied and the driving mechanism was attached to the top cap. The first target cell pressure was applied in stages while slowly releasing the suction pressure with the back open to the atmosphere. Once the target cell pressure had been reached and the consolidation process had been completed (measured using axial LVDTs), the back valve was closed and the resonant column tests were then performed under undrained conditions. The sand was tested at five different porosities, varying from the loose state to the dense state, and at isotropic effective stresses (σ_3') equal to 100, 300 and 500 kPa.

Table 1
Basic properties of the sand used in the study.

Type of sand	Fine-grained sand
Classification (USCS)	SP
Specific gravity (G_s)	2.69
Degree of roundness of particle	Angular
Maximum dry unit weight (γ_{dmax}) kN/m^3	16.58
Minimum dry unit weight (γ_{dmin}) kN/m^3	13.35
Maximum void ratio (e_{max})	0.97
Minimum void ratio (e_{min})	0.59
d_{10} (mm)	0.17
d_{30} (mm)	0.25
d_{60} (mm)	0.34
Uniformity coefficient, Cu	2.01
Coefficient of curvature, Cc	1.10
Percentage of minerals (X-ray diffraction analysis)	Quartz – 75 to 80% Feldspar – 18 to 23% Mica – 2%

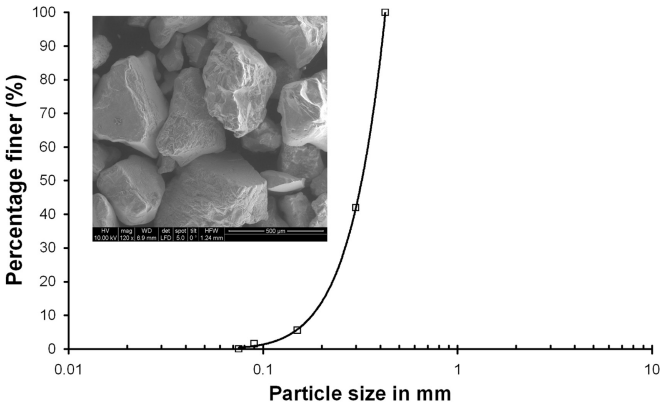

Fig. 1. Grading curve and SEM image of sand used in the study.

It is noted that most experimental works by the soil dynamics research community have focused on the shear stiffness of geomaterials as well as on material damping in the torsional mode, whereas the available data on Young's modulus of sands in longitudinal or flexural vibration are fairly limited. The successive measurement of Young's modulus is important since granular materials possess density and an effective stress-dependent Poisson's ratio due to inherent anisotropy (Kumar and Madhusudhan, 2010). In this direction, the study focuses on the behavior of sand in the flexural mode providing Young's modulus and material damping test results that evaluate the use of a new generation resonant column apparatus. The advantage of this technique is that, apart from the complete characterization of the dynamic properties of soils in the elastic-linear range of behavior, the modified Stokoe-type resonant column can be implemented in the evaluation of the strain-dependent elastic-plastic dynamic properties of geomaterials. This means that stiffness, material damping and dynamic Poisson's ratio as a function of shear strain can be obtained.

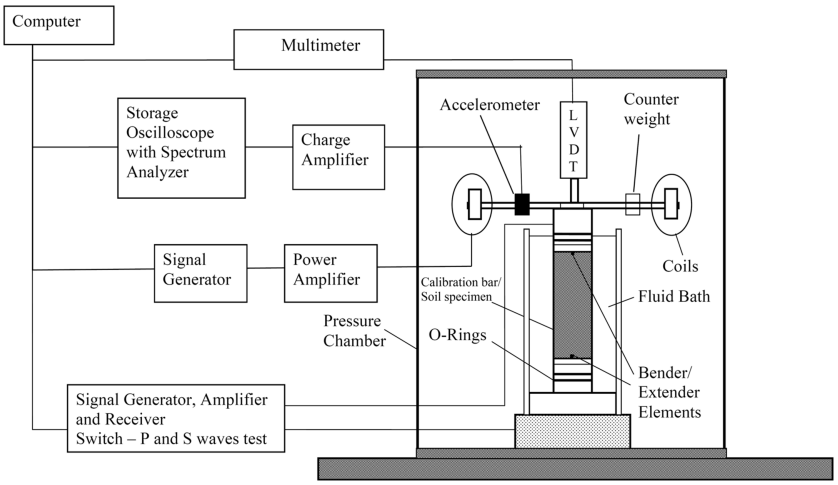

Fig. 2. Schematic of resonant column apparatus.

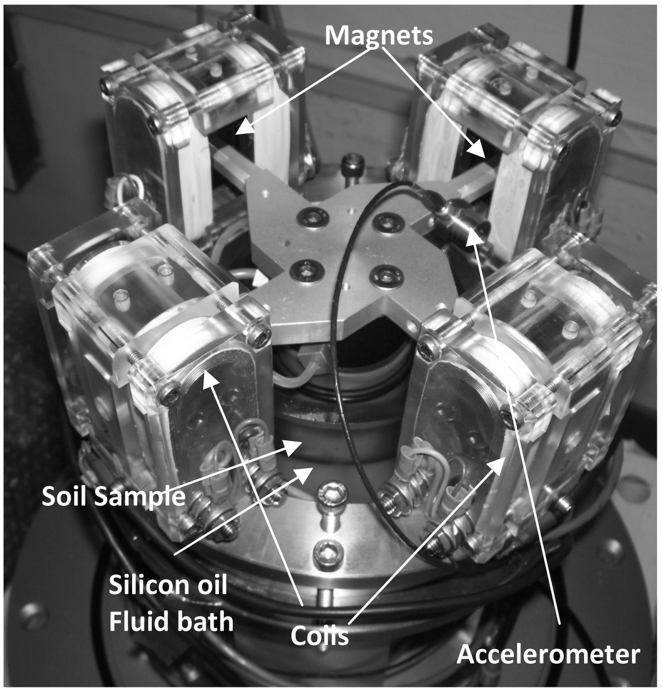

Fig. 3. Close-up view of the excitation mechanism.

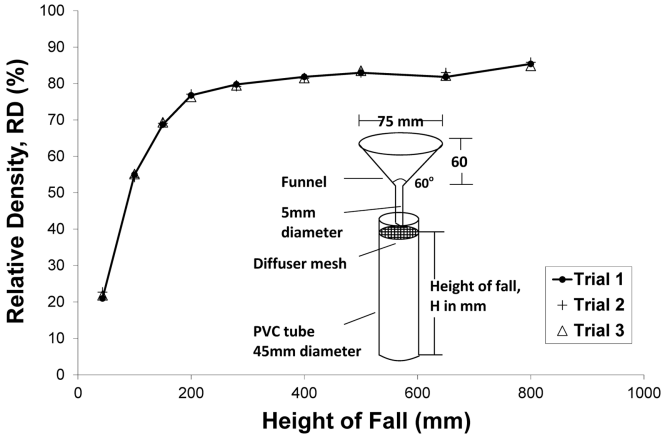

Fig. 4. Schematic of the pluviation device and calibration plot of relative density with height of fall.

3. Background of resonant column tests in flexural mode of vibration

In torsional resonant column tests, the shear modulus (G) and corresponding shear strain amplitude (γ) are determined in the first fundamental mode of vibrations using the standard expressions for fixed-free specimen end conditions (ASTM, 1992; Richart et al., 1970). In the flexural mode of vibration, Young's modulus (E) is obtained by considering the same fixed-free vibration analysis of a cantilever beam (soil sample) of length L, with a rigid mass at the free end, subjected to flexural bending. This method was proposed by Cascante et al. (1998), who adapted Rayleigh's method of mode shape analysis for the displacement in the first fundamental mode and obtained the solution as provided in Eq. (1).

$$\omega_f^2 = \frac{3 \times E \times I_b}{L^3 \times \left[\frac{33}{140} \times m_s + \sum_{i=1}^{N} \left(m_i \times f_i\right)\right]} \tag{1}$$

where ω_f is the circular resonant frequency, f_i is a non-dimensional function associated with mass m_i attached on top of the sample, which is defined in Eq. (2), m_s and L are the mass and the height of the sample, respectively, and I_b is the area moment of inertia of the sample about its longitudinal axis. In Eq. (2), $h0_i$ and $h1_i$ are the respective height to bottom and height to top of the individual mass attached on top of the soil specimen (Cascante et al., 1998).

$$f_i = 1 + \frac{3(h1_i + h0_i)}{2 \times L} + \frac{3\left(h1_i^2 + h0_i h1_i + h0_i^2\right)}{4 \times L^2} \tag{2}$$

The flexural strain is computed by averaging the measured displacement on top of the specimen over the entire cylindrical volume of the sample. The corresponding flexural strain, ε_f (expressed in percentile scale), for a given input voltage and the charge amplifier–accelerometer gain setting used to record

the displacement, is computed from Eq. (3).

$$\varepsilon_f = \frac{0.316 \times V \times R}{\{f_n^2 \times L \times [2 \times L + 3 \times (x_{accel} - L)]\}} \quad (3)$$

where V is the output from the accelerometer, R is the radius of the sample and x_{accel} is the vertical distance from the base of the sample to the center of the accelerometer.

In the study, the damping ratio for both flexural and torsional modes was determined using the free-vibration decay method (ASTM, 1992; Madhusudhan and Kumar, 2013). After attaining the resonant frequency in the torsion/flexure mode of vibrations, the sample is excited again at the resonant frequency, the input current supply to the coils is switched off in order to perform a free vibration test and the response of the accelerometer with time is recorded. During the free vibration of the sample, the amplitude decay curve with time is recorded from which the magnitude of the damping ratio is computed. Thereafter, the peak amplitude of each cycle is determined. The value of the logarithmic decrement, δ, and material damping, D, are then computed by the following expressions:

$$\delta = \frac{1}{n} log_e \frac{z_1}{z_{1+n}} \quad (4)$$

$$\delta = log_e \frac{z_1}{z_2} = \frac{2\pi D}{\sqrt{1 - D^2}} \quad (5)$$

where z_1 is the peak amplitude recorded for the first cycle, z_2 is the peak amplitude recorded for the second cycle, z_{n+1} is the peak amplitude recorded for the $(n+1)$th cycle and n is the number of cycles. After calculating the value of δ, the value of the damping ratio can be determined using Eq. (5). It is noted that three successive cycles were used during the free vibration of the sample for the material damping derivation in this study.

4. Calibration exercise of resonant column apparatus

Calibration of the resonant column in both torsional and flexural modes was performed in order to obtain the unknown parameters involved, such as, the mass polar moment of inertia of the drive mechanism (I_b). A calibration exercise was performed using aluminum bars and calibration weights and it was found that the shear and Young's moduli of the bars were very similar to the standard values, namely, in the range of 25.5–27.33 GPa ($G_{aluminum}$=26 GPa) and 63.31–65.84 GPa ($E_{aluminum}$=70 GPa), respectively, where $G_{aluminum}$ and $E_{aluminum}$ are the shear modulus and Young's modulus of the aluminum bar used in the calibrations. Typical results of the calibration exercise are given in Table 2. The resonant column apparatus used here works on the principle of the theory of vibration applied to the cantilever bar subjected to the first mode of vibration; and thus, the calibration and testing of soils is performed in the resonant frequencies within that range. For this reason, the size of the calibration bars is chosen in such a way that it matches the range in resonant frequency of the tested materials (soft soils to weak rocks) falling within the validity of the theory of vibration in the first fundamental mode by the apparatus for both torsional and flexural modes of vibration.

Table 2
Typical data of the calibration exercise in flexural and torsional modes of vibration.

Calibration bar thickness	Calibration weights (g)	E (MPa)	Flexural strain (%)	G (MPa)	Torsional strain (%)
10 mm	134.03	**64.45**	2.3×10^{-3}	25.74	3.3×10^{-4}
	268.09	**64.90**	2.6×10^{-3}	25.60	3.2×10^{-4}
	402.20	**63.31**	2.9×10^{-3}	25.49	3.5×10^{-4}
15 mm	134.03	**65.79**	8.4×10^{-3}	25.33	6.7×10^{-4}
	268.09	**64.90**	7.9×10^{-3}	26.55	6.7×10^{-4}
	402.20	**65.84**	6.4×10^{-3}	25.77	6.5×10^{-4}

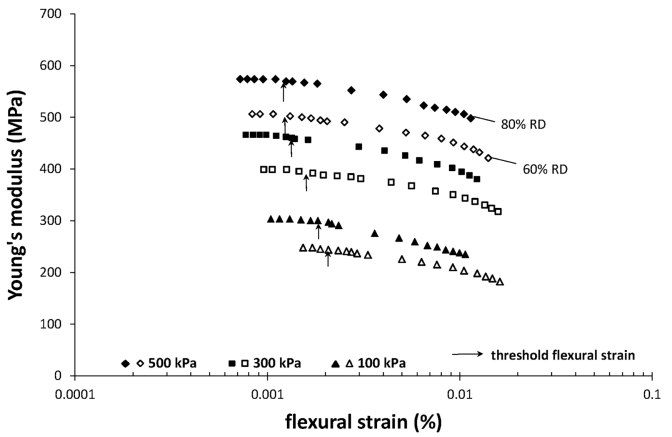

Fig. 5. Typical results of Young's modulus against flexural strain for samples SP2-60 and SP2-80.

5. Results of flexural excitation and associated Young's modulus

Typical plots of Young's modulus (E) against flexural strain (ε_f) for samples prepared at relative densities of 60% and 80% (denoted as SP2-60 and SP2-80, respectively) are shown in Fig. 5. E increased with an increase in confining stress σ_3' and the relative density. An increase in strain amplitude led to a gradual drop in E, and a more abrupt drop in stiffness was obtained for flexural strain beyond about 5×10^{-3}%. The figure also depicts the threshold strain (γ_t^e) beyond which the material no longer behaves as elastic. The threshold strain level of the material decreases with an increase in isotropic confining stress. In the study, γ_t^e was determined at E/E_0=0.99 (Vucetic, 1994), where E_0 is the elastic Young's modulus and E is the Young's modulus from small to large strains.

In Fig. 6, the elastic Young's moduli obtained from flexural resonant column tests are summarized and compared with the E_0 derived from extender element tests and an empirical-type model proposed by Saxena and Reddy (1989). Young's modulus values for sand, derived from flexural resonant column tests, agreed well with the results from the literature.

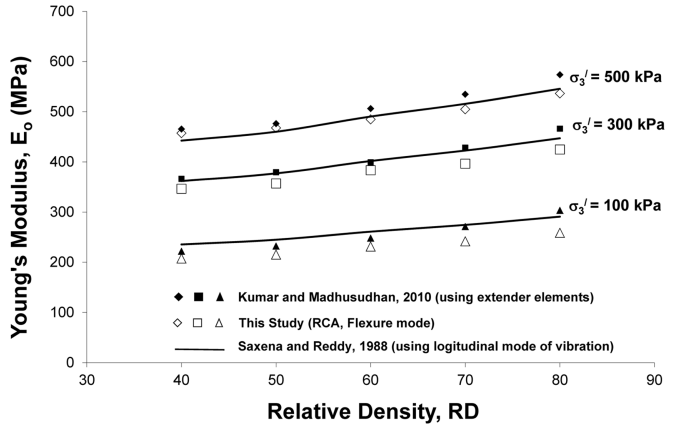

Fig. 6. Comparison of small-strain Young's modulus against relative density with results derived from extender element tests and empirical model.

It is noted that the results by Saxena and Reddy were obtained in the longitudinal resonant column mode of vibration. This means that in the present study and in the study by Saxena and Reddy (1989), Young's modulus was derived directly from sample resonance in the fundamental frequency of excitation, while the results derived from extender elements were based on the direct computation of primary waves (V_p) with a subsequent computation of constrained modulus (M_0) and Young's modulus (E_0) from (Eqs. (6)–8).

$$v = \frac{0.5 \times V_P^2 - V_S^2}{V_P^2 - V_S^2} \tag{6}$$

$$V_P = \sqrt{\frac{M_0}{\rho}} \tag{7}$$

$$M_0 = \frac{E_0 \times (1 - v)}{(1+v) \times (1 - 2 \times v)} \tag{8}$$

In the above equations, ρ is the mass density of the sample and v is Poisson's ratio derived from measurements of P-waves and S-waves using the bender/extender element inserts. The experimental results of Poisson's ratio, obtained by substituting wave velocities in Eq. (6), were reported in a previous work on the same sand by Kumar and Madhusudhan (2010). The values for Poisson's ratio are summarized in Table 3, wherein they indicate a reduction with an increase in stress and relative density.

The results of Fig. 6 are promising for the standardization of the flexural resonant column method. The advantage of the modified Stokoe-type resonant column of the study is that the stiffness measurements at variable modes of vibration and over a wide range of strain can be conducted. This allows us to capture the behavior of a soil sample in the elastic-linear range and in the non-linear elastic-plastic range. On the other hand, the bender/extender element inserts can provide stiffness measurements only at small levels of strain. This means that

Table 3
Typical Poisson's ratio values of the tested sand obtained from wave velocities using Eq. (6).

RD (%)	Poisson's ratio, ν		
	σ_3'= 100 kPa	σ_3' = 300 kPa	σ_3' = 500 kPa
40	0.23	0.191	0.161
50	0.231	0.186	0.157
60	0.227	0.178	0.152
70	0.223	0.170	0.147
80	0.219	0.163	0.142

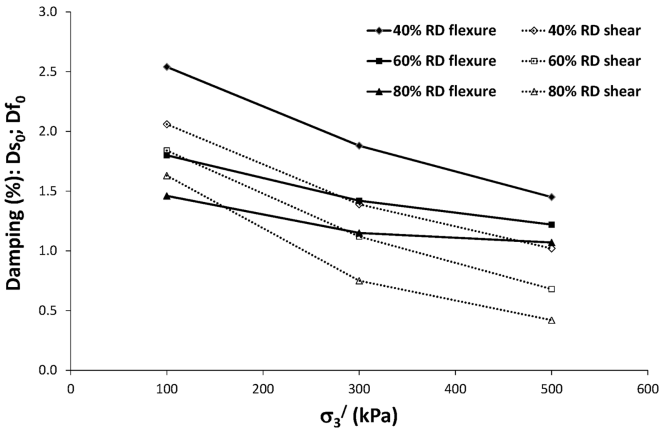

Fig. 7. Small-strain damping ratio for sands in torsional and flexural modes.

Poisson's ratio derivations can be obtained beyond the elastic-linear range of behavior which is invaluable for capturing the complete dynamic properties of geo-materials providing a complete geophysical characterization of soils.

6. Free decay response and associated flexural–torsional material damping

Typical comparisons of the small-strain damping ratio against isotropic stress (σ_3'), obtained in shear (Ds_0) and flexural (Df_0) modes of vibration, with reference to the smallest strain below the threshold strain, are illustrated in Fig. 7. Material damping decreased with an increase in σ_3' which is in agreement with previous works on granular soils, for example, Madhusudhan and Kumar (2013) and Senetakis et al. (2012). Flexure damping was found to be systematically higher in magnitude than shear damping for a given confining pressure and material state. At the lower confining stress level of 100 kPa, the ratio (Df_0)/(Ds_0) fell in the range of about 0.9 and 1.2, but for higher confining stress levels (i.e., 300 and 500 kPa), a greater decrease was observed in torsional damping than flexural damping with values of the ratio (Df_0)/(Ds_0) in the range of 1.3–2.0 (Fig. 8). Examples of typical free vibration decay data for torsional and flexural modes at small-

strains are presented in Fig. 9, for a given density and stress level (RD = 40% and σ_3' = 100 kPa). Notice the faster decay of amplitude in the flexural mode than in the torsional mode; this is because the frequency of the vibration in the flexural mode is 33 Hz, whereas in the torsional mode, it is 66.8 Hz.

For a given sample density, the increase in pressure leads to a decrease in damping, which is associated with faster wave propagation paths and a decrease in the attenuation of waves when the sample is subjected to greater pressure. This is because of the increase in grain contacts. Similarly, for a given stress level, a denser sample has lower material damping, because of the denser packing, an increase in grain contacts, and thus, a decrease in damping when the density increases (Madhusudhan and Kumar, 2013). When the sample is subjected to a flexural resonant column, wave propagation and particle perturbation along the axis of the sample dominate, whereas in the torsional mode, sample excitation is more global, i.e., waves propagate in the vertical direction and particle perturbation takes place in the horizontal plane. An increase in confining stress is expected to have a more pronounced effect on damping due to torsional excitation because of the more pronounced change in volumetric strain than axial strain. Assuming an isotropic material under isotropic conditions of confinement, we expect a volumetric strain equal to three times the axial strain. These more pronounced changes in volumetric strain than axial strain result in more a pronounced decrease in damping when the sample is vibrated in the torsional mode than in the flexural mode. The results in Fig. 7 verified this, whilst in a previous work by Saxena and Reddy (1989), comparisons between torsional and longitudinal damping showed a very similar trend.

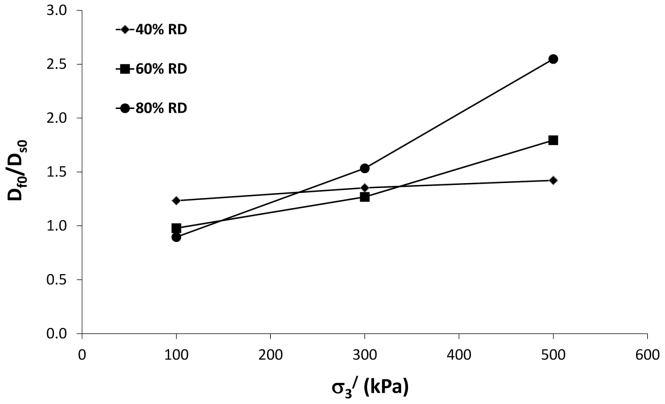

Fig. 8. Ratio of flexural to torsional damping.

7. Conclusions

In the study, the results of resonant column tests on quartz sand were reported which were obtained in the flexural mode of vibration using a modified Stokoe-type resonant column. The results, in terms of elastic Young's modulus, were compared with previously published data on the same sand using extender elements as well as an empirical type of model which was proposed based on the longitudinal mode of vibration resonant column tests. It was revealed that the comparison of Young's moduli using different experimental techniques was satisfactory. On the other hand, representative results on material damping in flexural and torsional modes were compared by adopting the free-vibration decay method. The results showed that material damping is sensitive to the mode of vibration. Flexural damping was higher in magnitude that shear damping and this trend was more pronounced at an increasing confining stress.

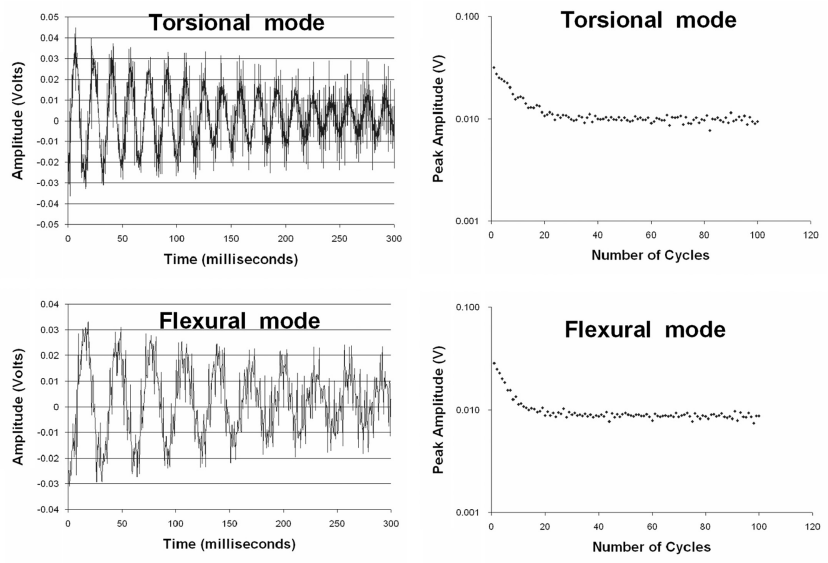

Fig. 9. Comparative free-vibration decay curves in torsional and flexural modes.

Acknowledgment

The authors would like to express their gratitude to the Indian Institute of Science, Bangalore for providing the facilities to carry out the experimental study.

References

ASTM, 1992. Standard test methods for modulus and damping of soils by the resonant column method: D4015-92. In: Annual Book of ASTM Standards, ASTM International.

Cascante, G., Santamarina, C., Yassir, N., 1998. Flexural excitation in a standard torsional-resonant column. Can. Geotech. J. 35, 478–490.

Clayton, C.R.I., 2011. Stiffness at small strain: research and practice. Geotechnique 61 (1), 5–37.

Kumar, J., Madhusudhan, B.N., 2010. Effect of relative density and confining pressure on Poisson ratio from bender and extender elements. Geotechnique 60 (7), 630–634.

Kumar, J., Madhusudhan, B.N., 2011. Dynamic Properties of sand from dry to fully saturated states. Géotechnique 62 (1), 45–54.

Lo Presti, D.C.F., Pedroni, S., Crippa, V., 1992. Maximum dry density of cohesionless soils by pluviation and by ASTM D 4253-83: a comparative study. Geotech. Test. J. 15 (2), 180–189.

Madhusudhan, B.N., Kumar, J., 2013. Damping of sands for varying saturation. J. Geotech. Geoenviron. Eng. (ASCE) 139 (9), 1625–1630.

Richart, F.E., Hall, J.R., Woods, R.D., 1970. Vibrations of soils and foundations. Prentice Hall, Englewood Cliffs, 414.

Saxena, S., Reddy, K., 1989. Dynamic moduli and damping ratios for Monterey No. 0 sand by resonant column tests. Soils Found. 29 (2), 37–51.

Senetakis, K., Anastasiadis, A., Pitilakis, K., 2012. The small-strain shear modulus and damping ratio of quartz and volcanic sands. Geotech. Test. J. 35 (6) http://dx.doi.org/10.1520/GTJ20120073.

Vucetic, M., 1994. Cyclic threshold shear strains in soils. J. Geotech. Eng. 120 (12), 2208–2228.